Available online at www.sciencedirect.com
ScienceDirect
Dyes and Pigments 79 (2008) 1–6
DYES and PIGMENTS
www.elsevier.com/locate/dyepig

Determination of the structure of 1,1′-diethyl-2,2′-carbocyanine iodide using NMR spectra and GIAO-HF/DFT calculations

Se-Mi Kim, Dong Hee Kim*

Department of Chemistry, Kunsan National University, 68 Miryong-Dong, Kunsan 573-701, South Korea

Received 25 October 2007; received in revised form 10 December 2007; accepted 14 December 2007
Available online 5 January 2008

Abstract

The chemical shift assignments of pinacyanol (1,1-diethyl-2,2′-carbocyanine) iodide were obtained by means of 1-D (^{1}H and ^{13}C) and 2-D (^{1}H–^{1}H COSY, ^{13}C–^{1}H COSY, and HMBC) NMR and theoretical calculations (GIAO-HF and GIAO-DFT using the 6-31+G(d,p) basis set). An optimized structure, calculated using B3LYP/6-31G(d), of the stable conformer gave a twist angle of $\gamma = 23.4°$ between the pairs of the quinoline planes, which was 0.4 kcal/mol lower than when $\gamma = 0°$. The (2*E*,12*E*) conformer having C_2 symmetry, matched well with the calculated and experimental ^{13}C and ^{1}H NMR chemical shifts in DMSO-d_6; GIAO-DFT provided better correlation ($R^2 = 0.997$, ^{13}C; $R^2 = 0.978$, ^{1}H) than GIAO-HF ($R^2 = 0.968$, ^{13}C; $R^2 = 0.949$, ^{1}H).

Keywords: Carbocyanine; PCYN; NMR spectroscopy; PES; GIAO-HF/DFT; Molecular structure

1. Introduction

Organic compounds that exhibit fluorescent activities have been studied extensively over the past century [1]. One group of such compounds consists of the carbocyanine dyes, which exhibit a variety of colors and commonly undergo photoisomerization. This special property has resulted in their use in the photographic industry as a spectral sensitizer [2,3]. They can also be applied in optoelectronics [4,5] and data storage [6,7], as molecular probes in biological systems [8,9], and in solar cells [10,11].

Pinacyanol (1,1-diethyl-2,2′-carbocyanine) iodide (PCYN), a member of the polymethine class of dyes (Fig. 1), was first used as a sensitizer in photography [3]. PCYN has also been used as a vital tool in staining leukocytes [12], in determining critical micelle concentrations [13], and as an indicator for solvent polarity due to its solvatochromic properties [14]. PCYN in aqueous solutions can undergo self-aggregation because of Van der Waals attractive forces between molecules. It has the ability to form bathochromic (J-aggregate, ‘‘brickwork’’ arrangement) or hypsochromic (H-aggregate, ‘‘card-pack’’ arrangement) aggregates [1,15,16], which is key to its photophysical characteristics. Despite its wide use, however, few experimental data have been reported based on the absorption, fluorescence, or Raman spectroscopy about some details of the conformation of PCYN [17,18].

NMR spectroscopy has proven to be an exceptional tool in the determination of molecular electronic structure and conformation. The shielding constants represent the most important source of structural information in high-resolution NMR [19]. With advances in NMR technology, two-dimensional (2-D) NMR spectroscopy can provide much additional information and efficiently assign proton or carbon NMR peaks in complex compounds such as the carbocyanine dyes. Unambiguous assignments of the ^{1}H and ^{13}C chemical shifts are made possible in the identification of proton and carbon signals, respectively, by analyzing 2-D correlation spectroscopy (COSY) [20] and heteronuclear multiple bond correlation (HMBC) [21].

Quantum chemical calculations of shielding constants can play an important role in the interpretation of measured chemical shifts in terms of the electronic and geometric structures. By establishing relationships between ^{1}H and ^{13}C NMR chemical shifts (δ, ppm) and absolute shielding tensors (σ, ppm), we

* Corresponding author. Tel.: +82 63 469 4576; fax: +82 63 469 4571.
E-mail address: dhkim@kunsan.ac.kr (D.H. Kim).

0143-7208/$ - see front matter © 2007 Elsevier Ltd. All rights reserved.
doi:10.1016/j.dyepig.2007.12.008

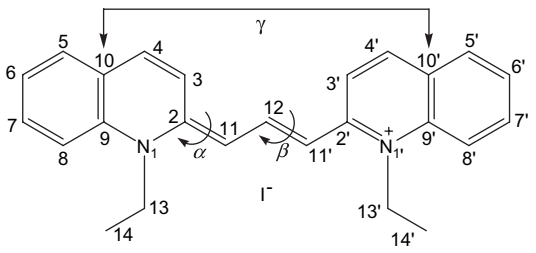

Fig. 1. Structure of PCYN with atom numbering. A number with a prime suffix denotes the equivalent atom in the other half of the molecule. α and β are dihedral angles about C3–C2–C11–C12′ and C11–C12–C11′–C2′, respectively, and γ is the dihedral angle for the pairs of the quinoline planes separated in space.

can efficiently assign or verify the consistency in the assignments of the NMR peaks [19]. Among several algorithms in the calculation of chemical shifts, gauge-including atomic orbital (GIAO) [22] approximation has been determined to be somewhat better than the others because it exhibits a faster convergence of the calculated properties on the extension of the basis set used [23]. This method has proven to be quite accepted and accurate, in particular when applied in the context of highly correlated *ab initio* methods, such as perturbation theory, especially when multiple bonds are present in the molecule. However, these methods are computationally demanding, even for modest-sized molecules. An effective alternative is the use of Density Functional Theory (DFT) that gives almost comparable results, but at a significantly lower computational cost [23–25].

The sensitivity of chemical shielding tensors to changes in the geometrical and electronic structures makes them an important source of information. The close correlation of the calculated ^{13}C and ^{1}H chemical shifts with the experimental values and high-level *ab initio* optimized geometries can serve as a tool in determining configurations and conformations of compounds [19].

This paper applied the GIAO-HF (Hartree–Fock) and GIAO-DFT methods to analyze the experimental ^{1}H and ^{13}C data of PCYN obtained by 1-D and 2-D NMR techniques. Also, we used different level of theories as a test for the quality of the calculation methods for NMR chemical shifts. The aim of this work is to give molecular structure of PCYN using the combined approach of NMR spectra and theoretical calculations of chemical shifts. To our knowledge, this paper appears to be the first attempt of determination of the molecular structure and investigation of ^{1}H and ^{13}C NMR spectra of PCYN in DMSO-d_6 solution.

2. Experimental

2.1. NMR spectroscopy

PCYN (98% purity) was purchased from Sigma–Aldrich Chemical Co. and was used as received. Solution ^{1}H and ^{13}C NMR spectra were recorded on Bruker DRX300 and DMX600 FT-NMR spectrometers at 25 °C and were processed using XWIN-NMR (Bruker Instruments, Inc.). Chemical shifts (δ, ppm) are given from the internal solvent, DMSO-d_6, 2.5 for ^{1}H and 39.5 for ^{13}C, with complex data points of 16 k and 64 k, respectively. Then 260–320 free induction decays (FIDs) of 2 k complex data points were collected for 2-D homonuclear COSY, ^{13}C–^{1}H heteronuclear COSY, and HMBC. For each FID, values from 16 to 50 scans were averaged, with repetition delays of 2–3 s. For the multiple bond correlation in HMBC analysis, 60 ms was used. FIDs were apodized using an exponential function for 1-D spectra and a squared sine-bell function for 2-D spectra, prior to Fourier transformation.

2.2. Computational methods

All quantum chemical calculations were carried out using the Gaussian 98 software package [26]. The ground-state geometry of the PCYN compound was fully optimized in vacuo without symmetry constraints with the *ab initio* HF self-consistent field (SCF) [27,28] and Becke's three-parameter hybrid functional (B3) [29] with the nonlocal Lee–Yang–Parr correlation (LYP) [30] theoretical methods; we applied the split-valence double-ζ basis set (6-31G) [31] with a single polarized function.

The PES scan for dihedral angles, α (C3–C2–C11–C12) and β (C11–C12–C11′–C2′) (Fig. 1), was carried out at 10° intervals in the range 0–360° at the HF level, with the 6-31G(d) basis set. Two stable conformers resulting from the PES scan were reoptimized at the DFT level using the B3LYP method with the 6-31G(d) basis set.

To determine the performance of various density functional methodologies and conventional HF-SCF procedures in predicting ^{1}H and ^{13}C isotropic chemical shifts from the 1-D and 2-D (COSY and HMBC) NMR spectroscopy of PCYN, GIAO NMR shielding tensors [32] were calculated using HF and DFT (B3LYP and B3 with Perdew and Wang's 1991 gradient-corrected (PW91) [29,33]) functionals with a singly-diffuse, doubly-polarized, split-valence double-ζ basis set (6-31+G(d,p)). ^{1}H and ^{13}C chemical shifts were then compared with tetramethylsilane (TMS) as the reference for chemical shielding, calculated with the same theoretical levels. The isotropic shielding constants, σ_i, were transformed to chemical shifts using $\delta_i = \sigma_{ref} - \sigma_i$, where σ_{ref} is the isotropic shielding of the reference compound.

3. Results and discussion

3.1. Geometry and PES scan

The PESs were calculated using HF/6-31G(d) as a function of the dihedral angles, α (C3–C2–C11–C12) and β (C11–C12–C11′–C2′) (Fig. 1), by rotating one C–C bond of the polymethine chain of PCYN (Fig. 2). Rotations around two of the C–C bonds yielded activation energy barriers of 12 and 6 kcal/mol for α and 17–18 and 12–14 kcal/mol for β. The sudden spike at −20° in the β rotation was due to the effect of steric hindrance between two hydrogen atoms (H_{C11} and $H_{C3'}$) having an interatomic distance of 1.94 Å. This is indicated by the difference in the dihedral angles

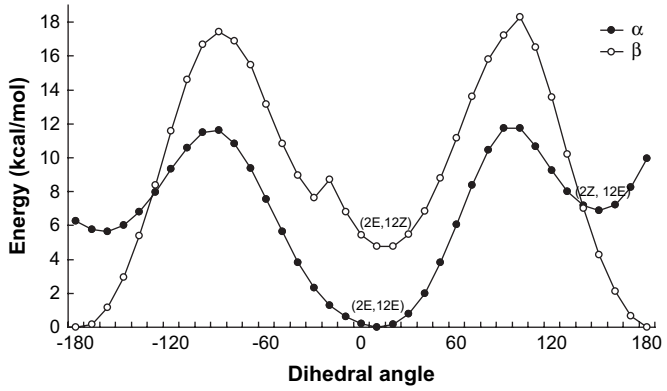

Fig. 2. Potential energy surface scan of the calculated relative energies using HF/6-31G(d) as a function of α and β dihedral angles.

(C2−C11−C12−C11′ and C11−C12−C11′−C2′) of 17.4° in HF/6-31G(d) and 20.9° in B3LYP/6-31G(d). Isomerization via β rotation around the bond connecting the polymethine chain to the terminal quinoline moiety was less favored, by about 6 kcal/mol, than α rotation (Fig. 2).

Using the *E/Z* notation, the geometries of the stable forms of PCYN, based on the PES scan, are (2*E*,12*E*), (2*E*,12*Z*), and (2*Z*,12*E*), where (2*E*,12*E*) is the most stable form, with a relative difference compared to the other conformers of 4.7 and 4.3 kcal/mol if calculated using HF/6-31G(d) and B3LYP/6-31G(d), respectively (Table 1). PCYN's most stable conformer (2*E*,12*E*) has a nonplanar conformation, with an equilibrium twist angle between the pairs of the quinoline planes, $\gamma = 23.4°$ at B3LYP/6-31G(d) level as shown in Fig. 3. This former is 0.4 kcal/mol lower than that of $\gamma = 0°$ by both the HF/6-31G(d) and B3LYP/6-31G(d) methods. The (2*E*,12*E*) conformer, with an overall structure that approaches C_2 symmetry, has nearly identical structures with equivalent bond lengths in each half, differing by only 0.08%. However, in the (2*E*,12*Z*) conformer, the two halves are somewhat asymmetric, with the largest bond length difference observed around the methine chain (Table 1). The biggest observed differences were at C2−C3 (C2′−C3′) and C2−C11 (C2′−C11′), with a difference of about 0.25% at BL3YP/6-31G(d). The optimized bond lengths calculated at HF/6-31G(d) show slight variations (<1%) from the B3LYP/6-31G(d)-optimized structure at the N1−C2 bond. Both HF and DFT methods gave equivalent bond lengths in each quinoline ring, to about two significant figures for HF and about three significant figures for B3LYP, suggesting that the (2*E*,12*E*) conformer assumes C_2 symmetry.

3.2. NMR spectroscopy and GIAO calculations

Figs. 4 and 5 respectively show the full range ^{13}C and ^{1}H NMR spectra of PCYN in DMSO-d_6. Fig. 4 indicates that the carbons of the polymethine chain have signals of 147.30 (C12) and 105.31 (C11) ppm. Signals for aromatic carbons were observed at 115.92−151.79 ppm, suggesting that the structure is symmetrical. Fig. 5 consists of well-defined proton signals from methyl and ethyl groups (−CH_3 and −CH_2−, at

Table 1
Geometrical parameters (in Å and degrees) of the two conformers of PCYN calculated at HF and B3LYP levels with 6-31G(d) basis set

Parameter	HF		B3LYP	
	(2*E*,12*E*)	(2*E*,12*Z*)	(2*E*,12*E*)	(2*E*,12*Z*)
E_{rel} (kcal mol^{-1})	0[a]	4.698	0[b]	4.280
Bond lengths				
N1−C2	1.356	1.359	1.383	1.382
C2′−N1′	1.356	1.351	1.383	1.381
C3−C2	1.440	1.442	1.434	1.433
C2′−C3′	1.440	1.432	1.433	1.430
C2−C11	1.410	1.406	1.417	1.418
C11′−C2′	1.409	1.423	1.417	1.422
C11−C12	1.387	1.398	1.395	1.399
C12−C11′	1.387	1.382	1.394	1.398
Bond angles				
C3−C2−C11	121.4	121.2	121.8	121.5
C11′−C2′−C3′	121.4	120.8	121.8	121.6
N1−C2−C11	121.2	121.4	121.0	121.2
C11′−C2′−N1′	121.2	121.0	121.0	120.7
C2−C11−C12	124.7	123.3	125.3	123.8
C12−C11′−C2′	124.7	128.0	125.3	128.2
C11−C12−C11′	123.8	131.4	123.6	130.2
Dihedral angles				
N1−C2−C3−C4	−1.4	−1.0	−1.6	−1.3
N1′−C2′−C3′−C4′	−1.4	0.0	−1.8	−0.6
C3−C2−C11−C12	11.4	16.5	10.2	18.3
C12−C11′−C2′−C3′	11.2	25.5	11.3	23.7
N1−C2−C11−C12	−169.4	−164.6	−170.9	−163.0
C12−C11′−C2′−N1′	−169.5	−158.4	−169.4	−160.4
C2−C11−C12−C11′	−177.2	−177.6	−176.6	−176.5
C11−C12−C11′−C2′	−177.1	15.0	−177.6	17.4

[a] Energy = −1069.98035774 Hartree.
[b] Energy = −1077.03955703 Hartree.

1.42 and 4.46 ppm, respectively), polymethine chain protons (protons 11, 11′, and 12 in the structure of PCYN) at 6.56 and 8.67 ppm, and a group of signals from aromatic protons between 7.43 and 8.28 ppm. The peaks at 3.2−4.5 ppm for

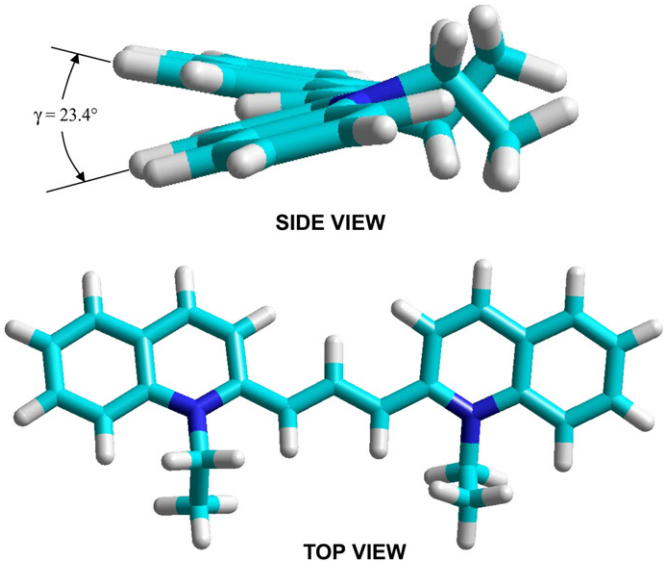

Fig. 3. Optimized structure of (2*E*,12*E*) conformer of PCYN calculated using B3LYP/6-31G(d).

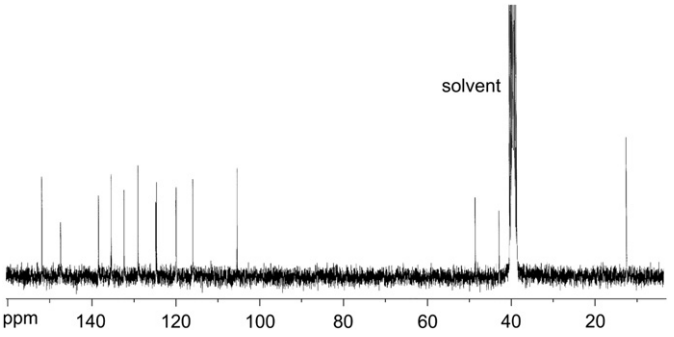

Fig. 4. The ^{13}C NMR spectrum of PCYN in DMSO-d_6 solution.

^{1}H and at 48.6 ppm for ^{13}C NMR were due to impurities. Full assignment of the ^{1}H and ^{13}C chemical shifts of PCYN was achieved using $^{1}H-^{1}H$ COSY, $^{13}C-^{1}H$ COSY, and $^{13}C-^{1}H$ HMBC experiments.

Comparison between experimental and theoretical NMR chemical shifts provides practical information on the chemical structure and conformation of compounds. This usefulness is largely due to empirical structure–chemical shift correlations. Based on the structural configuration of the (2*E*,12*E*) conformer of PCYN from theoretical calculations, the two halves, which are almost symmetric, should exhibit the same shielding tensors (Table 2). From Table 1, the difference in dihedral angles between C2–C11–C12–C11′ and C11–C12–C11′–C2′ for (2*E*,12*Z*) is about 21° using B3LYP/6-31G(d), whereas the difference is about 1° for the (2*E*,12*E*). The increase in dihedral angle in the methine chain from (2*E*,12*E*) to (2*E*,12*Z*) minimizes π-conjugation and thus increases the shielding on C11, C11′, and C12, as indicated by a decrease in the chemical shifts of about 2.5 ppm for both DFT methods.

The calculated ^{13}C NMR chemical shifts corresponded well with the PES scan, in which all calculations agreed with the (2*E*,12*E*) conformation being the stable structure for PCYN as indicated by no differences in the chemical shifts of C11 and C11′. This is because the increase in the dihedral angles minimized conjugation and thus increased the shielding effect on both C11 and C11′. As shown in Table 2, values derived from GIAO-DFT methods (B3LYP/6-31+G(d,p) and B3PW91/6-31+G(d,p)) are consistent with the ^{13}C NMR chemical shifts calculated with HF/6-31+G(d,p). The (2*E*,12*E*) conformation of PCYN was further confirmed

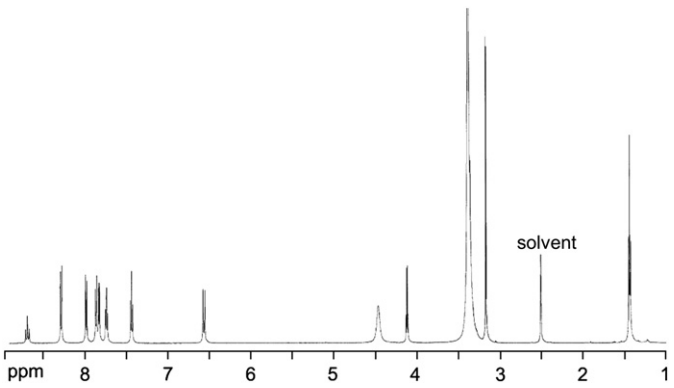

Fig. 5. The ^{1}H NMR spectrum of PCYN in DMSO-d_6 solution.

Table 2
Experimental and theoretical ^{13}C isotropic chemical shifts (in ppm) for the two conformers of PCYN calculated using the GIAO-HF and GIAO-DFT with 6-31+G(d,p) basis set

Atom	HF		B3LYP		B3PW91		Exp
	(2*E*,12*E*)	(2*E*,12*Z*)	(2*E*,12*E*)	(2*E*,12*Z*)	(2*E*,12*E*)	(2*E*,12*Z*)	
2	166.32	168.03	148.44	150.45	147.97	149.91	151.79
2′	166.42	169.08	148.46	149.80	148.00	149.29	
3	110.05	111.42	113.44	115.32	114.25	115.92	119.95
3′	110.14	115.44	113.57	119.15	114.36	119.76	
4	147.00	147.17	135.35	135.39	135.53	135.70	135.40
4′	147.10	148.11	135.34	135.28	135.52	135.62	
5	133.54	133.78	126.72	127.59	127.33	128.07	129.00
5′	133.55	133.49	126.57	128.00	127.15	128.47	
6	123.60	123.64	123.36	123.23	123.82	123.71	124.60
6′	123.66	124.27	123.49	123.27	123.95	123.72	
7	138.52	138.52	130.90	131.25	131.37	131.73	132.30
7′	138.55	138.97	130.96	131.36	131.44	131.84	
8	113.21	113.07	111.51	111.25	112.03	111.75	115.92
8′	113.24	113.82	111.52	112.12	112.07	112.48	
9	144.62	144.61	137.68	137.54	137.29	137.26	138.42
9’	144.59	144.75	137.64	138.09	137.24	137.82	
10	121.45	121.66	122.22	123.42	122.18	123.27	124.70
10′	121.49	121.96	122.19	123.22	122.15	122.94	
11	90.82	89.16	101.24	98.11	101.58	98.12	105.31
11′	90.87	87.13	101.21	99.07	101.55	99.50	
12	158.45	159.14	140.14	138.55	140.35	138.89	147.30
13	41.83	41.76	46.63	46.55	46.34	46.16	42.78
13′	41.84	42.51	46.68	48.44	46.38	48.14	
14	13.60	14.66	14.08	15.35	13.74	15.07	12.43
14′	13.63	13.73	14.09	13.95	13.74	13.62	

when compared with the results of ^{1}H NMR spectroscopy which showed that the molecule contained equivalent hydrogen atoms at H_{C11} and $H_{C11'}$, consistent with the C_2 symmetry of (2*E*,12*E*) (Table 3). Thus, ^{13}C and ^{1}H isotropic chemical shifts of the (2*E*,12*E*) conformation match well with

Table 3
Experimental and theoretical ^{1}H isotropic chemical shifts (in ppm) for the two conformers of PCYN calculated using the GIAO-HF and GIAO-DFT with 6-31+G(d,p) basis set

Atom	HF		B3LYP		B3PW91		Exp
	(2*E*,12*E*)	(2*E*,12*Z*)	(2*E*,12*E*)	(2*E*,12*Z*)	(2*E*,12*E*)	(2*E*,12*Z*)	
3	7.645	7.555	7.714	7.517	7.808	7.606	8.28
3′	7.645	8.190	7.729	8.013	7.823	8.096	
4	8.593	8.655	7.953	7.945	8.032	8.042	7.97
4′	8.608	8.738	7.951	7.981	8.029	8.081	
5	8.337	8.392	7.976	8.009	8.053	8.098	7.82
5′	8.343	8.424	8.001	7.928	8.078	8.027	
6	7.951	7.964	7.794	7.849	7.890	7.941	7.43
6′	7.956	8.032	7.783	7.881	7.880	7.970	
7	8.499	8.496	8.055	8.092	8.147	8.179	7.72
7′	8.505	8.571	8.073	8.175	8.163	8.249	
8	7.853	7.842	7.672	7.677	7.765	7.766	7.85
8′	7.856	7.987	7.690	7.803	7.780	7.880	
11	5.943	6.145	6.124	6.596	6.210	6.672	6.56
11′	5.948	5.283	6.129	5.805	6.214	5.908	
12	9.269	8.623	8.366	7.684	8.415	7.746	8.67
13	4.180	4.085	4.207	4.139	4.221	4.152	4.46
13′	4.180	4.282	4.213	4.355	4.227	4.377	
14	1.782	1.728	1.657	1.575	1.650	1.565	1.42
14′	1.786	1.776	1.661	1.613	1.655	1.599	

experimental values. This result demonstrates that PCYN mostly exhibits the (2*E*,12*E*) conformation, which assumes C_2 symmetry in DMSO-d_6 solution.

The quality of shielding constants depends on geometrical parameters [34] and on the method of calculation. *Ab initio* GIAO calculations showed a sensitivity of absolute nuclear shielding over the change in geometry, but the method used for GIAO calculations was more important than that used for the optimization of the geometry [35].

The inclusion of electron correlation effects should improve results for PCYN, a molecule containing π-conjugated carbons and a nitrogen atom. The improved results were clearly shown when the GIAO-HF and GIAO-DFT methods for the calculation of the chemical shifts were compared; the GIAO-DFT approach predicted the ^{13}C and ^{1}H chemical shifts of the aromatic rings in better agreement, within 3–6 ppm, with the experimental results than those calculated with GIAO-HF (1–15 ppm). The difference was particularly apparent at the C2 atom, a carbon atom bound to a nitrogen atom and a methine group. As shown in Table 2, the absolute error was about 15 ppm for the C2 atom using the GIAO-HF method compared to about 4 ppm using GIAO-DFT. Significant differences between the experimental and calculated ^{13}C NMR chemical shifts were also obtained for methine carbons (C11, C11′, and C12) in the polymethine chain: between 11 and 14 ppm for GIAO-HF and 4–7 ppm for GIAO-DFT. However, the quality of GIAO-HF was adequate for the assignment of aliphatic carbons such as C13 (C13′) and C14 (C14′). The absolute differences between the experimental and calculated values of these carbons were within 0.95–1.20 ppm for GIAO-HF and 1.31–3.90 ppm for GIAO-DFT (Table 2).

The following linear relationships were obtained for the (2*E*,12*E*) conformer:

^{13}C GIAO

HF: δ_{cal} (ppm) = $1.0679\delta_{exp} - 6.2112$ ($R^2 = 0.9683$)
B3LYP: δ_{cal} (ppm) = $0.9556\delta_{exp} + 3.0317$ ($R^2 = 0.9965$)
B3PW91: δ_{cal} (ppm) = $0.9589\delta_{exp} + 2.8120$ ($R^2 = 0.9970$)

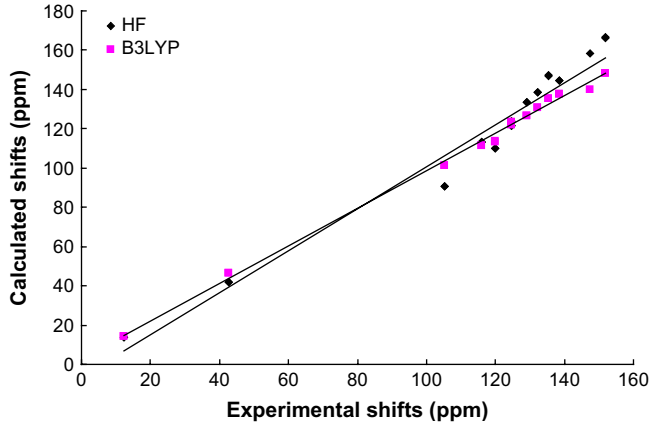

Fig. 6. Plot of the computed vs. experimental ^{13}C relative chemical shifts of PCYN for (2*E*,12*E*) conformer at GIAO-HF and GIAO-B3LYP with 6-31+G(d,p) basis set.

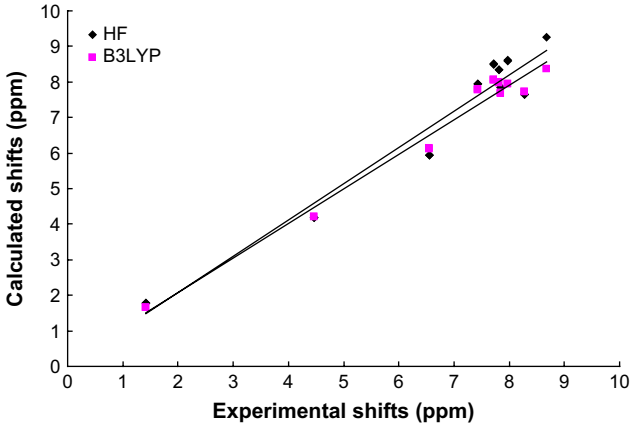

Fig. 7. Plot of the computed vs. experimental ^{1}H relative chemical shifts of PCYN for (2*E*,12*E*) conformer at GIAO-HF and GIAO-B3LYP with 6-31+G(d,p) basis set.

^{1}H GIAO

HF: δ_{cal} (ppm) = $1.0212\delta_{exp} + 0.0258$ ($R^2 = 0.9486$)
B3LYP: δ_{cal} (ppm) = $0.9714\delta_{exp} + 0.1425$ ($R^2 = 0.9781$)
B3PW91: δ_{cal} (ppm) = $0.9860\delta_{exp} + 0.1122$ ($R^2 = 0.9782$)

For the (2*E*,12*E*) conformer, the correlation graphs in the experimental ^{13}C and ^{1}H NMR and theoretical chemical shifts calculated by the GIAO-HF and GIAO-DFT methods are shown in Figs. 6 and 7, respectively. Linear relationships clearly exist between the theoretical and experimental carbon and proton chemical shifts for all the methods used.

The quality of the correlation could be considered as a test for the quality of calculation methods. For ^{13}C chemical shifts of the (2*E*,12*E*) conformer, the linear regression of all data (Fig. 6) showed a very good correlation with GIAO-B3LYP, giving a better correlation value and a smaller standard error ($R^2 = 0.9965$, SE = 2.31 ppm) than GIAO-HF ($R^2 = 0.9683$, SE = 7.92 ppm).

The performances of the B3LYP and B3PW91 DFT methods with respect to the prediction of the relative shieldings within the molecule were quite close. However, B3PW91/6-31+G(d,p) gave a slightly better coefficient and lower standard error ($R^2 = 0.9970$, SE = 2.14 ppm) than B3LYP/6-31+G(d,p) for ^{13}C chemical shifts. This trend of GIAO-DFT having a better correlation than GIAO-HF was also observed for the ^{1}H NMR chemical shifts, with the two GIAO-DFT methods having very similar correlation coefficients and standard errors ($R^2 = 0.978$, SE = 0.3). However, ^{1}H correlation coefficients were slightly smaller, by 0.02, than those of ^{13}C NMR chemical shifts.

4. Conclusions

Complete ^{1}H and ^{13}C NMR chemical shift assignments for PCYN were determined based on 1-D and 2-D ^{1}H–^{1}H COSY, ^{13}C–^{1}H COSY, and HMBC NMR experiments, coupled with theoretical calculations (GIAO-HF and GIAO-DFT). Three possible conformers were obtained based on the PES scan

method as a function of the dihedral angles, α (C3–C2–C11–C12) and β (C11–C12–C11′–C2′); the most stable conformer was (2*E*,12*E*), with a twist angle between the pair of quinoline planes of 23.4°, having C_2 symmetry. The calculated ^{13}C and ^{1}H NMR chemical shifts for the (2*E*,12*E*) conformer matched well with those obtained from 1-D and 2-D NMR experimental data, establishing the C_2 symmetry of the conformer in DMSO-d_6 solution.

Theoretical ^{13}C and ^{1}H chemical shift values (with respect to TMS) calculated with GIAO-DFT ($R^2 = 0.997$, ^{13}C; $R^2 = 0.978$, ^{1}H) were in significantly better agreement with the experimental values due to improved correlation effects than GIAO-HF ($R^2 = 0.968$, ^{13}C; $R^2 = 0.949$, ^{1}H). However, GIAO-HF was adequate for the assignment of aliphatic carbons and hydrogens (C13, C13′, and C14). Comparing the different GIAO-DFT methods, B3PW91 gave a slightly better correlation and smaller standard error against B3LYP for ^{13}C chemical shifts, but they were almost the same for ^{1}H chemical shifts.

References

[1] Mishra A, Behera RK, Behera PK, Mishra BK, Behera GB. Cyanines during the 1990s: a review. Chemical Reviews 2000;100(6):1973–2012.

[2] Adriaensen L, Vangaever F, Gijbels R. A comparative study of carbocyanine dyes measured with TOF-SIMS and other mass spectrometric techniques. Applied Surface Science 2004;231–232:348–52.

[3] West W, Carroll BH, Whitcomb DH. The adsorption of sensitizing dyes in photographic emulsions. Journal of Physical Chemistry 1952;56(9): 1054–67.

[4] Pugzlys A, Hania PR, Augulis R, Duppen K, van Loosdrecht PHM. Cylindrical aggregates of 5,5′,6,6′-tetrachlorobenzimidacarbocyanine amphiphilic derivatives: structure-related optical properties and exciton dynamics. International Journal of Photoenergy 2006;2006:1–9.

[5] Camposeo A, Persano L, Del Carro P, Virgili T, Cingolani R, Pisignano D. Polarization splitting in organic-based microcavities working in the strong coupling regime. Organic Electronics 2007;8(2–3):114–9.

[6] Morishima S-i, Warüshi K, Inagaki Y, Shibata M, Ishida T, Kubo H. A new type of light stabilizer for dye layers of optical disks: tetracyanoquinodimethane derivatives. Japanese Journal of Applied Physics 1999;38(3B):1634–7.

[7] Ricceri R, Abbotto A, Facchetti A, Pagani GA, Gabrielli G. Langmuir–Blodgett films of a new pyridium-dicyanomethanide dye and their potential optical applications. Langmuir 1997;13(13):3434–7.

[8] Kim BG, Dai H-N, McAtee M, Vicini S, Bregman BS. Labeling of dendritic spines with the carbocyanine dye DiI for confocal microscopic imaging in lightly fixed cortical slices. Journal of Neuroscience Methods 2007;162(1–2):237–43.

[9] Carreon JR, Stewart KM, Mahon Jr KP, Shin S, Kelley SO. Cyanine dye conjugates as probes for live cell imaging. Bioorganic and Medicinal Chemistry Letters 2007;17(18):5182–5.

[10] Burke A, Schmidt-Mende L, Ito S, Grätzel M. A novel blue dye for near-IR 'dye-sensitized' solar cell applications. Chemical Communications 2007;(3)::234–6.

[11] Zhan W-H, Wu W-J, Hua J-L, Jing YH, Meng FS, Tian H. Photovoltaic properties of new cyanine–naphthalimide dyads synthesized by 'Click' chemistry. Tetrahedron Letters 2007;48(14):2461–5.

[12] Makovitzky J, Bozsóky Jr S, László E. Topo-optical reactions of the human blood platelet membrane. Histochemistry and Cell Biology 1983;79(2):281–7.

[13] Sabate R, Gallardo M, de la Maza A, Estelrich J. A spectroscopy study of the interaction of pinacyanol with *n*-dodecyltrimethylammonium bromide micelles. Langmuir 2001;17(21):6433–7.

[14] Green MD, Patonay G, Ndou T, Warner IM. Spectroscopic effects of organized media on a cyanine dye/pyrene derivative. Journal of Inclusion Phenomena and Macrocyclic Chemistry 1992;13(2):181–93.

[15] Barazzouk S, Lee H, Hotchandani S, Kamat PV. Photosensitization aspects of pinacyanol H-aggregates. Charge injection from singlet and triplet excited states into SnO_2 nanocrystallites. Journal of Physical Chemistry B 2000;104(15):3616–23.

[16] Yonezawa Y, Ishizawa H. Luminescence properties of the mixed J-aggregate consisting of two kinds of thiacarbocyanine dyes or naphthothiacarbocyanine dyes having meso-substituent. Journal of Luminescence 1996;69(3):141–50.

[17] Du H, Fuh RCA, Li JZ, Corkan LA, Lindsey JS. PhotochemCAD: a computer-aided design and research tool in photochemistry. Photochemistry and Photobiology 1998;68(2):141–2.

[18] Werncke W, Tschol TJ, Weigmann HJ, Pfeiffer M, Lau A, Rentsch S, et al. Photoisomerization studies of pinacyanol using nanosecond time-resolved resonance cars. Journal of Raman Spectroscopy 1987;18(5):323–6.

[19] Kaupp M, Bühl M, Malkin VG. Calculation of NMR and EPR parameters: theory and applications. Weinheim: Wiley-VCH; 2004.

[20] Bax A, Freeman R. Investigation of complex networks of spin–spin coupling by two-dimensional NMR. Journal of Magnetic Resonance 1981;44:542–61.

[21] Bax A, Summers MF. Proton and carbon-13 assignments from sensitivity-enhanced detection of heteronuclear multiple-bond connectivity by 2D multiple quantum NMR. Journal of American Chemical Society 1986;108(8):2093–4.

[22] Ditchfield R. Self-consistent perturbation theory of diamagnetism. Molecular Physics 1974;27(4):789–807.

[23] Cheeseman JR, Trucks GW, Keith TA, Frisch MJ. A comparison of models for calculating nuclear magnetic resonance shielding tensors. Journal of Chemical Physics 1996;104(14):5497–509.

[24] Rablen PR, Pearlman SA, Finkbiner J. A comparison of density functional methods for the estimation of proton chemical shifts with chemical accuracy. Journal of Physical Chemistry A 1999;103(36):7357–63.

[25] Rauhut G, Puyear S, Wolinski K, Pulay P. Comparison of NMR shieldings calculated from Hartree–Fock and density functional wave functions using gauge-including atomic orbitals. Journal of Physical Chemistry 1996;100(15):6310–6.

[26] Frisch MJ, Trucks GW, Schlegel HB, Scuseria GE, Robb MA, Cheeseman JR, et al. Gaussian 98 Revision A.7. Pittsbugh, PA: Gaussian, Inc.; 1998.

[27] Roothaan CCJ. New developments in molecular orbital theory. Reviews of Modern Physics 1951;23(2):69–89.

[28] Pople JA, Nesbet RK. Self-consistent orbitals for radicals. Journal of Chemical Physics 1954;22(3):571–2.

[29] Becke AD. Density-functional thermochemistry. III. The role of exact exchange. Journal of Chemical Physics 1993;98(7):5648–52.

[30] Lee C, Yang W, Parr RG. Development of the Colle–Salvetti correlation-energy formula into a functional of the electron density. Physical Review B 1988;37(2):785–9.

[31] Rassolov VA, Ratner MA, Pople JA, Redfern PC, Curtiss LA. 6-31G* basis set for third-row atoms. Journal of Computational Chemistry 2001;22(9):976–84.

[32] Wolinski K, Hinton JF, Pulay P. Efficient implementation of the gauge-independent atomic orbital method for NMR chemical shift calculations. Journal of American Chemical Society 1990;112(23):8251–60.

[33] Perdew JP, Burke K, Wang Y. Generalized gradient approximation for the exchange-correlation hole of a many-electron system. Physical Review B 1996;54(23):16533–9.

[34] Lee MJ, Kim DH. Conformational study of liquid crystalline polymer: theoretical studies. Bulletin of the Korean Chemical Society 2006;27(1):39–43.

[35] Alkorta I, Elguero J. Ab initio (GIAO) calculations of absolute nuclear shieldings for representative compounds containing 1(2)H, 6(7)Li, 11B, 13C, 14(15)N, 17O, 19F, 29Si, 31P, 33S, and 35Cl nuclei. Structural Chemistry 1998;9(3):187–202.